The Madden-Julian Oscillation affects crop yields around the world

W.B. Anderson[1], E. Han[1], W. Baethgen[1], L. Goddard[1], Á.G. Muñoz[1], and A.W. Robertson[1]

[1]The International Research Institute for Climate and Society, Palisades, NY, United States

Key Points:

- The MJO affects maize yields in regions throughout the tropics and subtropics
- In dry, hot environments the MJO contributes to crop failures by reducing precipitation, decreasing soil moisture, and increasing extreme heat
- In sufficiently wet environments an MJO-induced decrease in rainfall reduces cloud cover, which increases solar radiation and benefits crop yields

Corresponding author: Weston Anderson, `weston@iri.columbia.edu`

Abstract

Understanding what causes weather-related stresses that lead to crop failures is a critical step towards stabilizing global food production. While there are many sources of weather-related stresses, the 30-60 day Madden-Julian Oscillation (MJO) is the dominant source of subseasonal climate variability in the tropics, making it a potential – but as of yet unexplored – source of crop failures. Here crop models and observational yield statistics are used to assess whether the MJO affects maize yields. We find that the influence of the MJO is widespread, affecting crop yields throughout the tropics. In dry, hot environments the MJO can lead to crop failures by reducing precipitation, decreasing soil moisture, and increasing extreme heat, while in wetter, cooler environments – where water stress is less common – MJO-forced decreases in rainfall bring increases in solar radiation that benefits crop yields. These results provide a pathway to develop actionable early warnings using subseasonal forecasts.

1 Introduction

Crop yields in rainfed cropping systems, which account for $> 75\%$ of cropped areas globally (Portmann et al., 2010), depend not only on seasonal total rainfall and temperature, but also on the distribution of that rain and heat within the growing season (Prasad et al., 2008). Exposure to extreme heat, even on the timescale of just hours to days, can significantly damage crop yields (Schlenker & Roberts, 2009), particularly when it occurs during sensitive stages of crop development (Prasad et al., 2008). These extreme climate events may be relatively short in duration but they often occur with little warning and are spatially widespread enough to affect global-scale food production (Lesk et al., 2016). In the coming decades climate change will accelerate the frequency and severity of climate extremes (Teixeira et al., 2013), making mitigating the effects they have on food production critical.

Preventing crop failures associated with extreme climate requires understanding what causes those conditions in the first place. Climate extremes can have any number of dynamical origins, from interannual variability associated with e.g. the El Niño Southern Oscillation (Iizumi et al., 2014; Anderson et al., 2019) to synoptic weather systems (Ray et al., 2015). Distinguishing between the two is critical when considering how to build a climate-smart food production system. While abiotic stresses arising from weather systems may only be predictable up to a week or two in advance, extreme climate conditions attributable to predictable modes of variability, like the El Niño Southern Oscillation, may be anticipated and acted upon using seasonal climate forecasts (Goddard & Dilley, 2005). In between the predictable seasonal and weather time scales, however, is a nascent source of climate information for agriculture and food production: the 30-60 day Madden Julian Oscillation (MJO).

As the dominant source of subseasonal climate variability in the tropics (Madden & Julian, 1972; Zhang, 2005), the MJO represents a significant opportunity for agricultural climate services. While MJO activity levels vary from year-to-year, an active MJO organizes tropical atmospheric circulation at planetary scales into regions of enhanced and suppressed convection. Deep convection associated with the MJO often first appears over the Indian Ocean and propagates eastward, reaching the western Pacific about two weeks later. The surface expression of the MJO dissipates as it continues east over the cold sea surface temperatures in the eastern Pacific before reforming in the tropical Atlantic.

The circumglobal path of the MJO means that it potentially has a far-reaching relevance to global rainfed agriculture. The MJO influences the West African (Lavender & Matthews, 2009; Matthews, 2004), Indian (Joseph et al., 2009; Pai et al., 2011), Asian (Lawrence & Webster, 2002), and Australian (Wheeler et al., 2009) monsoons. It affects precipitation in East Africa (Pohl & Camberlin, 2006b, 2006a; Berhane & Zaitchik, 2014),

southwest Asia (Barlow et al., 2005; Nazemosadat & Ghaedamini, 2010), South America (Grimm, 2019; Valadão et al., 2017), and southern Mexico (Barlow & Salstein, 2006). But to date, despite progress understanding the often-large impacts of the MJO on rainfall, its physical mechanisms, and improvements to MJO forecasts (Pegion et al., 2019), the impacts of the MJO on agriculture are still largely unknown. Here, for the first time, we analyze whether a single MJO event can affect crop yield statistics and whether the effect of the MJO is detectable in historical crop yields. We focus our analysis on maize because an active MJO has been shown to affect precipitation, soil moisture, and extreme maximum temperatures throughout the tropics during the maize flowering season (Anderson et al., accepted), which is when grain crops are particularly sensitive to abiotic stresses (Prasad et al., 2008; Barnabás et al., 2008). Our results provide a pathway to develop actionable early warnings of climate hazards and their impacts using subseasonal forecasts.

2 Materials and methods

2.1 Data

To identify MJO teleconnections we use daily interpolated station-based temperature data, and daily precipitation and soil moisture products that blend satellite and station data. We use daily soil moisture estimates from the Global Land Evaporation Amsterdam Model (GLEAM) v3.2a (1981-2016), which uses satellite-observed surface (0-10 cm) soil moisture, vegetation optical depth, reanalysis air-temperatures and a multi-source precipitation product to derive surface soil moisture values (Martens et al., 2017). Daily precipitation data comes from the Climate Hazards group Infrared Precipitation with Stations (CHIRPS; 1981-2016) at 0.25 degrees (Funk et al., 2015). We use values of daily maximum and minimum temperature at 2m from the Berkeley Earth dataset (1981-2016), which is a one-degree gridded interpolation-based statistical product (Rohde et al., 2013), and daily solar insolation from the ranalysis-based NASA-POWER (1983-2013) agroclimatology dataset (Stackhouse et al., 2015). To construct weather forcing for the DSSAT crop model we use data from the common period of 1983-2013.

We use observational crop statistics at the national and subnational scale to estimate the effects of the MJO on regional crop yields. Subnational crop statistics were downloaded for India from the Directorate of Economics and Statistics (https://eands.dacnet.nic.in/); for Mexico from the INEGI Information Databank (http://www3.inegi.org.mx/sistemas/biinegi/); for Brazil we use first-season maize only from the Brazilian Companhia Nacional de Abastecimento (CONAB; http://www.conab.gov.br/index.php); data for the rest of Central America, West Africa and East Africa was only available at a national scale and was downloaded from the Food and Agriculture Organization FAOSTAT database (http://www.fao.org/faostat/en/).

To calculate crop yield anomalies we first remove the long-term trend using a low-pass Gaussian filter with a kernel density of three years, which is similar to a nine-year running mean. Deviations from this "expected yield" are absolute yield anomalies. We calculate percent yield anomalies as the absolute yield anomaly divided by the expected yield for each subnational district. Regional yield anomalies are calculated by using observed harvested areas to calculate regional percent yield anomalies. As a sensitivity experiment, we recalculated the results based on yield anomalies derived from a five-year running mean but found little difference.

2.2 Daily climate anomalies

We estimate the impact of harmful increases in maximum temperature around flowering by counting degree-days above a critical temperature threshold (T_c), which in this case is 29° C for maize (Schlenker & Roberts, 2009). Our temperature threshold is chosen to identify detrimental, not necessarily lethal, temperatures (Schlenker & Roberts,

2009; Sánchez et al., 2014). During the three months prior to harvest, which is defined for each point using the Sacks et al. (2010) data, the number of 'extreme degree days' (EDD) were then calculated as follows:

$$EDD = \sum_{i=1}^{n} max(0, T_{max,i} - T_c)$$

where $T_{max,i}$ is the maximum temperature on the ith day of the flowering period (that lasts n days). We use an average of daily EDDs across all years to define the climatology of EDDs.

For the non-derived variables of soil moisture and precipitation, we define the climatology using the first three harmonics. Daily anomalies are similarly calculated as departures from this daily climatology and calculated for MJO events during the three months prior to harvest .

2.3 MJO event identification

To identify MJO teleconnections, we create composites of all days (1981-2016) in which the Wheeler-Hendon Realtime Multivariate MJO (RMM) indices, which measure MJO activity (Wheeler & Hendon, 2004), have an amplitude of greater than one standard deviation. We mask out all areas in which there are fewer than 1000 observations in the climate dataset or where maize is not cultivated. Measuring MJO teleconnections is straightforward in Southwest Mexico and Central America, Northeast Brazil, and East Africa, where the MJO influences crop growing conditions is directly related to the eastward propagating convection anomalies. In each of these areas we plot composites of damaging maximum temperatures and soil moisture anomalies by MJO phase in Figure 2 below. MJO teleconnections in West Africa and India, on the other hand, are at least partly the result of Rossby and Kelvin waves that propagate away from the main envelope of deep convection associated with the MJO. In West Africa teleconnections are primarily a response to westward propagating Rossby waves generated by MJO-related convection (Vigaud & Giannini, 2019; Lavender & Matthews, 2009; Matthews, 2004). Over India in the summer, the eastward propagating MJO acquires a northward propagating component that reaches the 10-25N region up to two weeks later (Lawrence & Webster, 2002; Wang et al., 2018).

To capture the integrated effect of these teleconnections we plot the cumulative sum of soil moisture and extreme degree-day anomalies during ten-day windows corresponding to the expected timing of teleconnections for each phase: days 0-10 and 5-15 for West Africa and India, respectively. We choose the timing of the lag based on previous literature demonstrating the time it takes for MJO-forced waves to propagate to our points in West Africa (Lavender & Matthews, 2009; Matthews, 2004; Vigaud & Giannini, 2019) and India (Lawrence & Webster, 2002). For all other regions we show instantaneous teleconnections.

2.4 DSSAT model simulation

To simulate MJO teleconnections to maize yields we use the DSSAT crop model (Hoogenboom et al., 2019; J. W. Jones et al., 2003; C. A. Jones, 1986), run at specific spatial locations. We choose locations that (1) are maize production regions and (2) in which the MJO-teleconnections at a single point is representative of the average MJO teleconnection to the entire region as a whole (Fig. 3). This ensures continuity between our point-based simulation of yields and regional analysis of climate teleconnections. For each chosen location, we performed a literature review to identify an appropriate cultivar and parameterization for the model (Jagtap et al., 1999; Justino et al., 2013; Babel & Turyatunga, 2015; Royce, 2002). Parameters from regionally-relevant field trials were used where available (SI Table 1). Where no such data was available, as was the

case in Mexico, we relied on expert elicitation. We next identify suitable soils in the WISE soils database, and calibrate the model planting date based on observational yield statistics. For each location we use three planting dates to simulate variable sowing decisions, and choose two soil profiles to represent different likely soil conditions (SI Table 1).

We force the DSSAT crop model with observed daily precipitation, incoming solar radiation, and maximum and minimum temperature to create series of baseline crop yield simulations in each location. We next create a weather forcing ensemble to measure the marginal effect of an MJO event on crop yield anomalies. We use the same MJO events from our composite analysis described in Sect 2.3 to create the ensemble. For each day in which the MJO was active in a given phase during crop flowering, we select the maximum temperature, minimum temperature, solar radiation and precipitation for that day and the following two weeks to account for propagating waves and persistent teleconnections. To estimate the marginal effect of one MJO event on crop yields, we overwrite two weeks of observed weather in the DSSAT forcing file around the time of flowering (as determined in the DSSAT calibration runs) with the "MJO event weather" and re-run DSSAT with the perturbed weather forcing. For the purposes of generating a large ensemble, each historical MJO event in a particular phase is inserted at the flowering time, regardless of when it occurred in the observed record. We then repeat this process for all possible combinations of MJO events, years, three planting dates, and two soils to produce an ensemble of size (# events)x(# years)x(# planting dates)x(# soils) for each phase of the MJO. This creates an ensemble of over 300,000 yield anomalies for each region (>40,000 per phase per region). Finally, we calculate the marginal effect of each MJO event by differencing the DSSAT crop yield with the added "MJO event weather" from the DSSAT crop yield forced by observed weather without the added event.

To identify the effect of each MJO phase on crop yields, we use multi-linear regression to regress the MJO phase of each forcing event onto the calculated crop yield anomalies while controlling for the year into which that event was inserted:

$$\delta Y_{ij} = Ph_i + Yr_j \tag{1}$$

where δY_{ij} is the crop yield anomaly in year j forced by MJO event i, Yr_j is a fixed effect for each year to remove interannual variability, and Ph_i is a series of dummy variables corresponding to the phase of the MJO during each event i. In this way we both remove interannual variability and isolate the average expected influence of an individual MJO event on crop yield anomalies.

2.5 Effect of the MJO in observational crop statistics

Our regression onto simulated yield anomalies can provide us with an estimate of the potential influence of any single MJO event that begins in a particular phase on crop yields. But it does not tell us whether these effects are present in observational yield statistics. Because we cannot isolate the effect of individual MJO phases in the observational record, as we did with our DSSAT simulations, we instead take a counterfactual approach and ask "do bad yield years and good yield years show a difference in the frequency of events in particular MJO phases?". To answer this question we use both our DSSAT ensemble and observational records.

In our DSSAT ensemble for each location, we identify the highest and lowest 10,000 yield anomalies, which is roughly the top and bottom 2.5% of the distribution, and record the Realtime Multivariate MJO (RMM) index values associated with each MJO event used to produce those yield anomalies in the DSSAT ensemble. We then create two probability density functions of MJO activity in an RMM diagram, one for the events associated with the "good years" and one for the events associated with the "bad years". The difference of these two distributions indicates the relative frequency of MJO phases that

produced good yields and those that lead to bad yields. If there is no difference between the two distributions, then the MJO has no discernible influence. If there is a difference, however, then the relative frequencies can be compared to our climate analysis to check for consistency.

We repeat this process with observational yields by selecting subnational or national units within each region, and aggregating yields into a single regional value. We next identify the high and low terciles of crop yields in the region, and for each year we identify the daily MJO phases and amplitudes during the maize growing season (Jun - Sep for India, May-Sep for Southwest Mexico, May-Aug for West Africa, Apr-Sep for East Africa, and both Feb-May and Sep-Dec for cropping seasons in Northeast Brazil). We again take the difference between the distribution of daily MJO RMM indices during high and low yield terciles to calculate the difference in MJO activity between good and bad years.

3 Results

3.1 MJO Teleconnections

Dry and hot teleconnections tend to persist for around 15 days (Fig. 1), which is sufficient to depress seasonal total maize yields (Schlenker & Roberts, 2009). The temperature-stress pathway is likely to be largest in Northeast Brazil, West Africa, and India where teleconnections to extreme temperatures are strongest.

Using a large ensemble of modeled crop yields, we separate the effect of the MJO from that of both seasonal variability (e.g. the El Niño Southern Oscillation) and random weather. We find that the MJO affects maize yields throughout the tropics, but that its influence is stronger in Northeast Brazil and India than in other regions studied (Fig. 2). Each MJO event, of which there may be multiple during a given growing season, affects maize yields by $\sim$0.5 - 1%.

3.2 Regional dynamics

MJO impacts on Southwest Mexico and Northeast Brazil are phased similarly. Large-scale descent in phases 3-6 suppress convection (Fig. 1), which, after a few days, dries out the soil and leads to increased maximum air temperatures. During phases 7-2, on the other hand, westerly winds advect moisture into Southwest Mexico (Barlow & Salstein, 2006) and large-scale convection over Northeast Brazil leads to precipitation (Valadão et al., 2017), which wets the soils and cools maximum air temperatures.

Despite the similarity of the MJO teleconnections to the climate in these two regions, the effect on crop yields is quite different due to differing growing conditions. Our modeled point in Northeast Brazil is arid and hot, which means that maize is regularly exposed to heat stress and drought. Our point in Southwest Mexico, on the other hand, is relatively wet and cool, such that maize is exposed to less extreme temperatures (Fig. 1) and is water-stressed much less often in the DSSAT simulations (SI Figure 1). Wet, cool conditions in Northeast Brazil during phases 7-2, therefore, generally increase crop yields, while the hot, dry conditions in phases 3-6 decrease crop yields (Fig. 2). In Southwest Mexico, clear skies bring an increase in solar radiation that tends to improve yields, while increased precipitation decreases solar radiation and leads to lower crop yields on average.

An MJO event being sufficient to affect modeled crop yields doesn't demonstrate that the effect is necessarily seen in observed yields. After all, the MJO is only one of many factors that affect crop yields in these regions. To test whether the effect of the MJO is present in observational statistics we analyzed whether the frequency or intensity of the MJO during the growing season systematically differs during good and poor harvest years (see Methods).

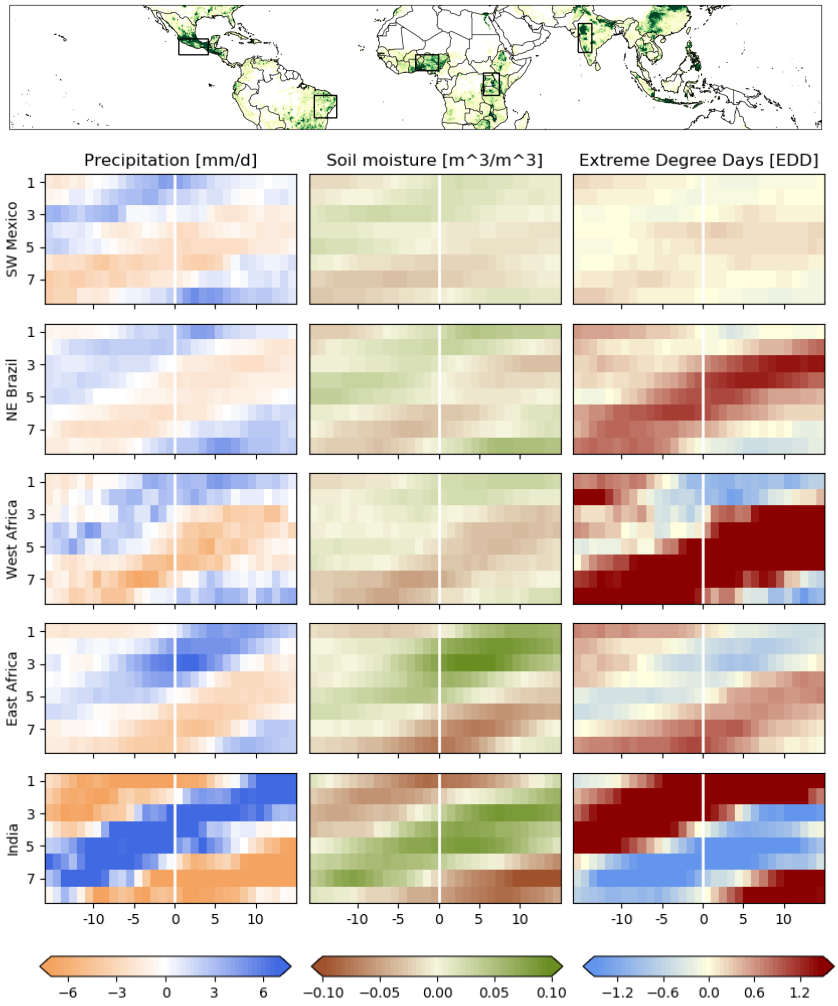

Figure 1. Average precipitation, soil moisture, and extreme degree-day anomalies during days with an active MJO for each phase (1-8; y-axis) from 15 days before an event occurs to 15 days after an event occurs (x-axis). Values are averaged over each region shown by the boxed area in the top panel, which shows maize growing locations. Propagation of the MJO is indicated by the slope of anomalies in the phase-lag plot.

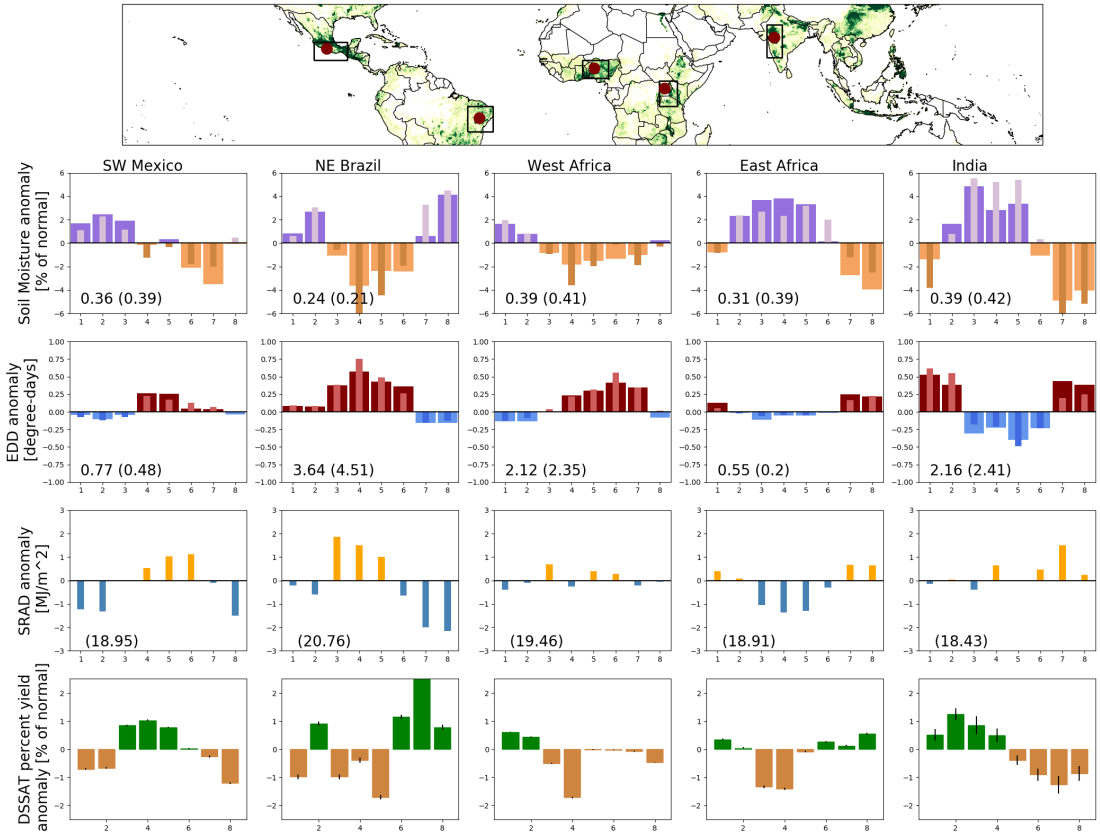

Figure 2. Average soil moisture, extreme degree-day, solar radiation, and modeled maize yield anomalies associated with an active MJO event for each phase (x-axis) in each region. Anomalies of incident solar radiation are for point data only. Each region is shown in black boxes while each point used to simulate crop yields within the region is shown in red (top panel). Thick bars in each panel indicate regional-averages, while thin bars indicate anomalies at the point used to simulate crop yields. Numbers in each panel indicate regional climatologies around flowering for volumetric soil moisture (in m^3/m^3), extreme degree days, and incident solar radiation ($MJ/m^2/day$), while numbers in parentheses indicate climatologies at each point.

In Northeast Brazil, years with poor maize yields are associated with increased MJO activity in phases 2-5 during the growing season, while years with good maize yields are associated with increased MJO activity in phases 6-1 (Fig. 3). The frequency of MJO events in good and bad years based on observational statistics match results based on our DSSAT model ensemble to first order (SI Fig. 2), although there are differences between the two distributions of MJO activity. These results are consistent with our climate analysis for the region, in which dry, hot MJO teleconnections lower maize yields while wet, cool MJO teleconnections improve maize yields (Fig. 2).

In Southwestern Mexico the observational ensemble indicate that years with poor crop yields are associated with phases 7-2 (Fig. 3), although the DSSAT ensemble indicates that poor crop yields are associated with MJO phases 6-8 (Fig. 2 and SI Fig 2). The discrepancy between modeled and observed results may be due to the difference between the area-averaged statistics and the DSSAT point estimate, or it may reflect a discrepancy between the modeled and historical cropping practices in the region. Further research is needed to more precisely characterize how MJO-related variations in the growing season climate of Southwest Mexico translates into variations in crop yields.

The MJO affects maize yields in West Africa primarily via a remote response to MJO activity in the Indian Ocean. When the MJO enhances convection in the Indian Ocean and suppresses convection in the West Pacific warm pool (phases 1-2) it generates an atmospheric equatorial Kelvin wave that travels east and equatorial Rossby waves that travel west, which reach West Africa about a week later, destabilizing the atmospheric column, and enhancing rainfall in the region (Lavender & Matthews, 2009; Matthews, 2004). Accordingly, phases one and two are characterized by increased precipitation (Fig. 1), wet soils, an absence of high temperatures and above expected crop yields (Fig. 2). Phases 3-6 are associated with dry, hot conditions that lower modeled crop yields. Phase four is most damaging to crop yields in West Africa, possibly because as the MJO tends to propagate from phase 4-8, teleconnections are consistently dry and hot, prolonging the time before rain provides relief to the crop. These results are consistent with good harvests in the observational statistics being associated with an increase in MJO phases 7-2, while poor harvests are associated with increased activity in MJO phases 3-6 (Fig. 3). Similarly, the good yielding years in the model ensemble are associated with an increase in the frequency of phases 1-2 and a decrease in the frequency of phases 3-4, although the effect of phases 5-8 are muted in the modeled results as compared to the observational statistics.

In the East African highlands, precipitation anomalies are controlled by the atmospheric stability conditions imposed by the MJO (Pohl & Camberlin, 2006b, 2006a; Berhane & Zaitchik, 2014). During phases 2-5 large-scale deep convection is responsible for wet, cool conditions. Similar to Southwest Mexico, however, the growing conditions at our modeled point in Uganda are cool and wet, such that increased precipitation decreases incoming solar radiation and decreases modeled maize yields (Fig. 2). These DSSAT results, however, must be interpreted with the understanding that many regions – but particularly East Africa – are a complex mosaic of agro-climates and soils, which will result in a non-homogenous crop yield response to a homogenous MJO-forced climate anomaly. In observational crop yield statistics, differences in the frequency of MJO phases in good vs poor yield years are noisy, perhaps due to the lack of available, reliable, subnational crop yield data or due to the complex crop growing environment in the region. While there is reasonable agreement between the modeled maize yields and observed yields, no strong conclusions about observed East African maize yields can be drawn based on Figure 3.

In India, precipitation anomalies are associated with meridionally propagating Rossby waves triggered by the eastward-moving deep-convective anomalies of the MJO (Lawrence & Webster, 2002). Large-scale convective anomalies over the Indian Ocean propagate northward over the course of 1-2 weeks into the 15-25N region (Lawrence & Webster,

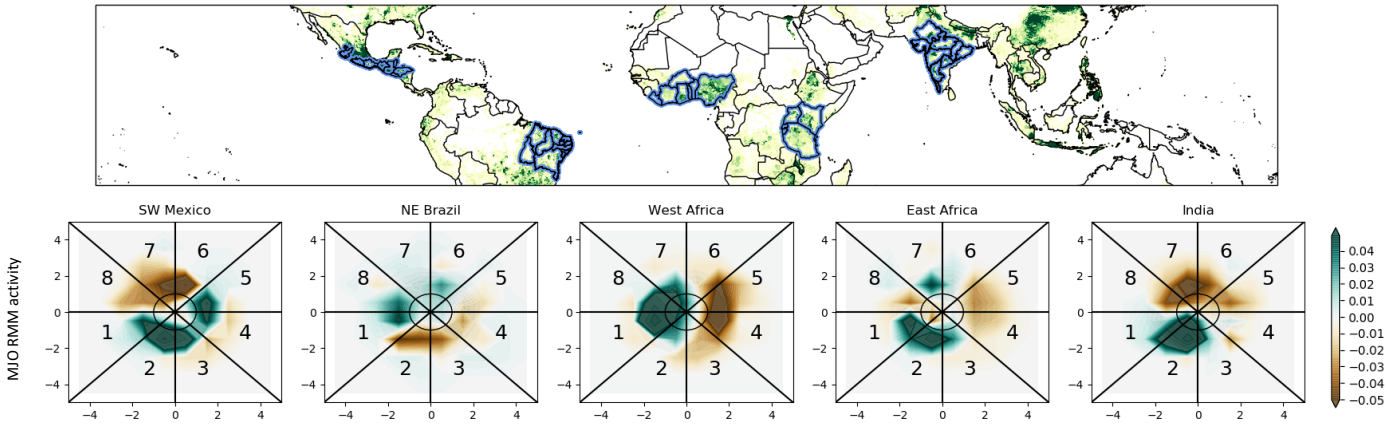

Figure 3. Differences between MJO activity in good yield and poor yield years as measured by the normalized, 2-dimensional probability density functions of the RMM indices during the months prior to harvest. Subnational or national units included in each region for observational statistics are shown in blue in the top panel. Good yield years are identified as the top-tercile of regional yields, while poor yield years are bottom-tercile years. The difference between the distributions of RMM indices in good yield and poor yield years is statistically significant at the 5% level in all cases.

2002), where most maize is cultivated in India. Increased deep convection over the Indian ocean in phases 1-4 leads to increased precipitation 1-2 weeks later, which leads to wet soils and, after a few days, cool air temperatures over the maize growing regions of India (Fig. 1). Accordingly, phases 1-4 lead to increased maize yields in model simulations (Fig. 2) and increased MJO activity in phases 1-4 is associated with years of good maize harvests in both the observational data and model simulations (Fig. 3). Phases 5-8, which are associated with suppressed convection over the Indian Ocean, lead to dry, hot conditions (Joseph et al., 2009; Moron et al., 2012; Pai et al., 2011) and below-expected maize yields (Figs. 2 and 3).

4 Discussion

A historical example of when the MJO likely affected crop yield anomalies was the 2002 monsoon season in India. At the time, the 2002 drought was among the worst in over a century despite seasonal forecasts for normal monsoon rainfall (Bhat, 2006). The drought in July, when the MJO was strongly active in phases 6-8 (SI Fig. 3), had a large contribution from intraseasonal disturbances (Bhat, 2006; Kripalani et al., 2004), although a developing El Niño likely played a role in the drought as well via cross-timescale interactions (Muñoz et al., 2015). The spatial pattern of maize yield anomalies in 2002 matches well what would be expected from MJO-forced extreme heat in phases 6-8 (SI Fig. 3). Reduced maize yields in India following MJO activity in phases 6-8 is furthermore consistent with both our observational and modeled analyses (Figs. 1-3). The 2002 drought illustrates how intraseasonal forcing may play a role in even the most intense crop failures.

Our results more generally demonstrate that the MJO affects crop yield variations throughout the tropics. In dry, hot environments the MJO forces crop failures by reducing precipitation, decreasing soil moisture, and increasing extreme heat while in wetter, cooler environments – where water stress is less common – MJO-forced decreases in rainfall bring an increase in solar radiation that benefits crop yields. We find that each MJO event affects final crop yields by $\sim$0.5 - 1% of expected yields, although multiple events may occur in a single season. For reference, the 2002 drought in India led to the worst maize growing season in recent history, with national yields reduced by around 17% compared to the previous year (FAO, 2009). Average MJO reductions in crop yields on the order of one percent per event, therefore, are non-negligible contributions to crop failures even measured against the most devastating yield losses.

But a number of open questions remain. Our results indicate that one path by which the MJO may affect final crop yields is through an increased frequency of some MJO phases relative to others. It is also possible, however, that a nonlinear crop yield response to excess heat could rectify onto the end-of-season crop yields even when the MJO propagates through both cool phases that improve yields and hot phases that decrease yields. Further research is needed to fully understand the mechanisms by which the MJO affects crop yields.

The ability to attribute crop failures to the MJO provides a new incentive to glean operational value from our rapidly improving understanding of subseasonal climate. Current forecast models can now forecast the MJO with high skill up to 4 weeks in advance (Vitart, 2017) and – in some of the regions analyzed – subseasonal forecasts of precipitation demonstrate skill at lead times of up to three weeks (Pegion et al., 2019). Such forecasts could be used to extend weather forecasts to inform agricultural decisions. Doing so would represent a significant advance for climate-smart agriculture by providing users with a continuum of actionable forecasts from the weather to seasonal time scales. Using subseasonal forecasts to anticipate false starts to the rainy season, for example, could help inform the timing of crop planting to prevent crop failures.

Owing to the effects of the MJO on climate extremes during grain crop flowering seasons on virtually every continent (Anderson et al., accepted), there is good reason to believe that the MJO has widespread relevance to global agriculture. Better understanding how the MJO affects crop yields may lead to significant advances in monitoring and predicting food production shortfalls.

Acknowledgments

This project was supported by ACToday, a Columbia World Project. W.B.A acknowledges funding from the Earth Institute Postdoctoral Fellow Program. ÁGM was partially supported by the NOAA award NA18OAR4310275. AWR was supported by a fellowship from Columbia University's Center for Climate and Life. We would like to thank Kai Sonder and Jim Hansen for discussions about how to parameterize the crop model, and Zane Martin for helpful discussions about the MJO. All climate and crop yield statistics used in this paper are publicly available from the links specified in the Methods section. All information needed to reproduce the DSSAT crop yields is supplied in Table S1.

References

Anderson, W., Muñoz, Á. G., Goddard, L., Baethgen, W., & Chourio, X. (accepted). MJO teleconnection to crop growing seasons. *Climate Dynamics*.

Anderson, W., Seager, R., Baethgen, W., Cane, M., & You, L. (2019). Synchronous crop failures and climate-forced production variability. *Science advances*, *5*(7), eaaw1976.

Babel, M., & Turyatunga, E. (2015). Evaluation of climate change impacts and adaptation measures for maize cultivation in the western uganda agro-ecological zone. *Theoretical and applied climatology*, *119*(1-2), 239–254.

Barlow, M., & Salstein, D. (2006). Summertime influence of the madden-julian oscillation on daily rainfall over mexico and central america. *Geophysical research letters*, *33*(21).

Barlow, M., Wheeler, M., Lyon, B., & Cullen, H. (2005). Modulation of daily precipitation over southwest asia by the madden–julian oscillation. *Monthly weather review*, *133*(12), 3579–3594.

Barnabás, B., Jäger, K., & Fehér, A. (2008). The effect of drought and heat stress on reproductive processes in cereals. *Plant, cell & environment*, *31*(1), 11–38.

Berhane, F., & Zaitchik, B. (2014). Modulation of daily precipitation over east africa by the madden–julian oscillation. *Journal of Climate*, *27*(15), 6016–6034.

Bhat, G. S. (2006). The indian drought of 2002—a sub-seasonal phenomenon? *Quarterly Journal of the Royal Meteorological Society: A journal of the atmospheric sciences, applied meteorology and physical oceanography*, *132*(621), 2583–2602.

FAO. (2009). *Food and agriculture organization statistical databases.*

Funk, C., Peterson, P., Landsfeld, M., Pedreros, D., Verdin, J., Shukla, S., ... others (2015). The climate hazards infrared precipitation with stations—a new environmental record for monitoring extremes. *Scientific data*, *2*, 150066.

Goddard, L., & Dilley, M. (2005). El Niño: catastrophe or opportunity. *Journal of Climate*, *18*(5), 651–665.

Grimm, A. M. (2019). Madden–julian oscillation impacts on south american summer monsoon season: precipitation anomalies, extreme events, teleconnections, and role in the mjo cycle. *Climate Dynamics*, 1–26.

Hoogenboom, G., Porter, C., Shelia, V., Boote, K., Singh, U., White, J., ... Jones, J. (2019). *Decision support system for agrotechnology transfer (dssat) version 4.7.5* (Tech. Rep.). Gainesville, Florida, USA.: DSSAT Foundation.

Iizumi, T., Luo, J.-J., Challinor, A. J., Sakurai, G., Yokozawa, M., Sakuma, H., ...

Yamagata, T. (2014). Impacts of El Niño Southern Oscillation on the global yields of major crops. *Nature communications*, *5*.

Jagtap, S., Abamu, F., & Kling, J. (1999). Long-term assessment of nitrogen and variety technologies on attainable maize yields in Nigeria using CERES-maize. *Agricultural systems*, *60*(2), 77–86.

Jones, C. A. (1986). *Ceres-maize; a simulation model of maize growth and development* (Nos. 04; SB91. M2, J6.).

Jones, J. W., Hoogenboom, G., Porter, C. H., Boote, K. J., Batchelor, W. D., Hunt, L., ... Ritchie, J. T. (2003). The dssat cropping system model. *European journal of agronomy*, *18*(3-4), 235–265.

Joseph, S., Sahai, A., & Goswami, B. (2009). Eastward propagating MJO during boreal summer and indian monsoon droughts. *Climate Dynamics*, *32*(7-8), 1139–1153.

Justino, F., Oliveira, E. C., de Ávila Rodrigues, R., Gonçalves, P. H. L., Souza, P. J. O. P., Stordal, F., ... others (2013). Mean and interannual variability of maize and soybean in Brazil under global warming conditions. *American Journal of Climate Change*, *2*(04), 237.

Kripalani, R., Kulkarni, A., Sabade, S., Revadekar, J., Patwardhan, S., & Kulkarni, J. (2004). Intra-seasonal oscillations during monsoon 2002 and 2003. *Current Science*, 325–331.

Lavender, S. L., & Matthews, A. J. (2009). Response of the west african monsoon to the madden–julian oscillation. *Journal of Climate*, *22*(15), 4097–4116.

Lawrence, D. M., & Webster, P. J. (2002). The boreal summer intraseasonal oscillation: Relationship between northward and eastward movement of convection. *Journal of the atmospheric sciences*, *59*(9), 1593–1606.

Lesk, C., Rowhani, P., & Ramankutty, N. (2016). Influence of extreme weather disasters on global crop production. *Nature*, *529*(7584), 84.

Madden, R. A., & Julian, P. R. (1972). Description of global-scale circulation cells in the tropics with a 40–50 day period. *Journal of the atmospheric sciences*, *29*(6), 1109–1123.

Martens, B., Gonzalez Miralles, D., Lievens, H., Van Der Schalie, R., De Jeu, R. A., Fernández-Prieto, D., ... Verhoest, N. (2017). Gleam v3: Satellite-based land evaporation and root-zone soil moisture. *Geoscientific Model Development*, *10*(5), 1903–1925.

Matthews, A. J. (2004). Intraseasonal variability over tropical africa during northern summer. *Journal of Climate*, *17*(12), 2427–2440.

Moron, V., Robertson, A. W., & Ghil, M. (2012). Impact of the modulated annual cycle and intraseasonal oscillation on daily-to-interannual rainfall variability across monsoonal india. *Climate dynamics*, *38*(11-12), 2409–2435.

Muñoz, Á. G., Goddard, L., Robertson, A. W., Kushnir, Y., & Baethgen, W. (2015). Cross–time scale interactions and rainfall extreme events in southeastern south america for the austral summer. part i: Potential predictors. *Journal of Climate*, *28*(19), 7894–7913.

Nazemosadat, M., & Ghaedamini, H. (2010). On the relationships between the madden–julian oscillation and precipitation variability in southern iran and the arabian peninsula: Atmospheric circulation analysis. *Journal of Climate*, *23*(4), 887–904.

Pai, D., Bhate, J., Sreejith, O., & Hatwar, H. (2011). Impact of mjo on the intraseasonal variation of summer monsoon rainfall over india. *Climate Dynamics*, *36*(1-2), 41–55.

Pegion, K., Kirtman, B. P., Becker, E., Collins, D. C., LaJoie, E., Burgman, R., ... others (2019). The subseasonal experiment (subx): A multi-model subseasonal prediction experiment. *Bulletin of the American Meteorological Society*(2019).

Pohl, B., & Camberlin, P. (2006a). Influence of the madden–julian oscillation on east african rainfall: Ii. march–may season extremes and interannual vari-

ability. *Quarterly Journal of the Royal Meteorological Society*, *132*(621), 2541–2558.

Pohl, B., & Camberlin, P. (2006b). Influence of the madden–julian oscillation on east african rainfall. i: Intraseasonal variability and regional dependency. *Quarterly Journal of the Royal Meteorological Society*, *132*(621), 2521–2539.

Portmann, F. T., Siebert, S., & Döll, P. (2010, March). MIRCA2000-Global monthly irrigated and rainfed crop areas around the year 2000: A new high-resolution data set for agricultural and hydrological modeling. *Global Biogeochemical Cycles*, *24*(1). Retrieved from `http://doi.wiley.com/10.1029/2008GB003435` doi: 10.1029/2008GB003435

Prasad, P., Staggenborg, S., & Ristic, Z. (2008). Impacts of drought and/or heat stress on physiological, developmental, growth, and yield processes of crop plants. *Response of crops to limited water: Understanding and modeling water stress effects on plant growth processes*(responseofcrops), 301–355.

Ray, D. K., Gerber, J. S., MacDonald, G. K., & West, P. C. (2015). Climate variation explains a third of global crop yield variability. *Nature communications*, *6*, 5989.

Rohde, R., Muller, R., Jacobsen, R., Perlmutter, S., Rosenfeld, A., Wurtele, J., ... Mosher, S. (2013). Berkeley earth temperature averaging process. *Geoinformatics & Geostatistics: An Overview*, *1*(2), 1–13.

Royce, F. S. (2002). *A systems approach to enso-based crop management with applications in argentina, costa rica and mexico* (Unpublished doctoral dissertation). University of Florida.

Sacks, W. J., Deryng, D., Foley, J. A., & Ramankutty, N. (2010). Crop planting dates: an analysis of global patterns. *Global Ecology and Biogeography*, *19*(5), 607–620.

Sánchez, B., Rasmussen, A., & Porter, J. R. (2014). Temperatures and the growth and development of maize and rice: a review. *Global change biology*, *20*(2), 408–417.

Schlenker, W., & Roberts, M. J. (2009). Nonlinear temperature effects indicate severe damages to us crop yields under climate change. *Proceedings of the National Academy of sciences*, *106*(37), 15594–15598.

Stackhouse, P. W., Westberg, D., Hoell, J. M., Chandler, W. S., & Zhang, T. (2015). Prediction of worldwide energy resource (power)-agroclimatology methodology-(1.0 latitude by 1.0 longitude spatial resolution). *Technical Report of NASA Langley Research Center and SSAI/NASA Langley Research Center*, 1–46.

Teixeira, E. I., Fischer, G., Van Velthuizen, H., Walter, C., & Ewert, F. (2013). Global hot-spots of heat stress on agricultural crops due to climate change. *Agricultural and Forest Meteorology*, *170*, 206–215.

Valadão, C. E., Carvalho, L. M., Lucio, P. S., & Chaves, R. R. (2017). Impacts of the madden-julian oscillation on intraseasonal precipitation over northeast brazil. *International Journal of Climatology*, *37*(4), 1859–1884.

Vigaud, N., & Giannini, A. (2019). West african convection regimes and their predictability from submonthly forecasts. *Climate Dynamics*, *52*(11), 7029–7048.

Vitart, F. (2017). Madden—julian oscillation prediction and teleconnections in the s2s database. *Quarterly Journal of the Royal Meteorological Society*, *143*(706), 2210–2220.

Wang, S., Ma, D., Sobel, A. H., & Tippett, M. K. (2018). Propagation characteristics of bsiso indices. *Geophysical Research Letters*, *45*(18), 9934–9943.

Wheeler, M. C., & Hendon, H. H. (2004). An all-season real-time multivariate mjo index: Development of an index for monitoring and prediction. *Monthly Weather Review*, *132*(8), 1917–1932.

Wheeler, M. C., Hendon, H. H., Cleland, S., Meinke, H., & Donald, A. (2009). Impacts of the madden–julian oscillation on australian rainfall and circulation.

519 *Journal of Climate*, *22*(6), 1482–1498.
520 Zhang, C. (2005). Madden-julian oscillation. *Reviews of Geophysics*, *43*(2).